Case Studies in Thermal Engineering 43 (2023) 102688

Contents lists available at ScienceDirect

Case Studies in Thermal Engineering

journal homepage: www.elsevier.com/locate/csite

Thermal evaluation of a room coated by thin urethane nanocomposite layer coating for energy-saving efficiency in building applications

AliAkbar Azemati [a,b], Seyed Saeid Rahimian Koloor [c], Hossein Khorasanizadeh [a], GhanbarAli Sheikhzadeh [a], Behzad Shirkavand Hadavand [d,*], Mohamed Eldessouki [c,e,f,**]

[a] Department of Thermo Fluids, Faculty of Mechanical Engineering, University of Kashan, Kashan, Iran
[b] Department of Mechanical Engineering, Abadan Branch, Islamic Azad University, Abadan, Iran
[c] Institute for Nanomaterials, Advanced Technologies and Innovation (CXI), Technical University of Liberec (TUL), Studentská 1402/2, 460 01, Liberec, Czech Republic
[d] Institute for Color Science and Technology, Department of Resin and Additives, Tehran, Iran
[e] Empa, Swiss Federal Laboratories for Materials Science and Technology, Laboratory for Biomimetic, Membranes and Textiles, St. Gallen, Switzerland
[f] Faculty of Engineering, Mansoura University, Mansoura, Egypt

ARTICLE INFO

Handling Editor: Huihe Qiu

Keywords:
Thermal simulation
Nanocomposite coating
Thermal conductivity
Energy-saving
Radiant cooling
Finite volume method

ABSTRACT

Today, it is common to use thin-layer nanocomposite coatings as insulation to reduce heat loss through building walls. One of the important advantages of these coatings is preventing energy loss as a thermal barrier in low thicknesses and with high efficiency. Investigations on the energy loss and saving of coated buildings are often practiced using numerical and experimental approaches. In this study, numerical simulation and experimental evaluation consisting of modification of nanoparticles and preparation powder coating nanocomposite, are used to study the effects of coated polyurethane nanocomposite containing nano Al_2O_3 and nano ZrO_2 on both sides of the walls of a sample room on temperature distribution and heat transfer. For this purpose, a three-dimensional enclosure was assumed as a room having a radiant cooling panel, which is modeled under various features of the walls' interior and exterior coating. To determine the flow and temperature fields, the governing equations that include the continuity, momentum, turbulence, and energy equations, which are coupled through the buoyancy term, have been solved using the Fluent software. The SIMPLE algorithm to accommodate the pressure-velocity coupling, the k-ε model for turbulence modeling, the Boussinesq approximation for buoyancy term modeling, and the DO model for radiation simulation, are employed. The results of the thermography of the samples showed that the temperature reduction in the samples containing zirconium oxide compared to aluminum oxide had a better performance in the thermal insulation of the coating and the lowest temperature was observed in the nanocomposite containing 3% zirconium oxide. Numerical studies showed that this thin layer nanocomposite coating reduces

* Corresponding author.
** Corresponding author. Empa, Swiss Federal Laboratories for Materials Science and Technology, Laboratory for Biomimetic, Membranes and Textiles, St. Gallen, Switzerland.
E-mail addresses: shirkavand@icrc.ac.ir (B.S. Hadavand), eldesmo@auburn.edu (M. Eldessouki).

https://doi.org/10.1016/j.csite.2022.102688
Received 30 January 2022; Received in revised form 19 December 2022; Accepted 29 December 2022
Available online 31 December 2022

energy consumption by 4% and 13%, respectively, compared to pure polyurethane coatings and acrylic paints.

Nomenclature

A	*Area (m^2)*
b	*Wall thickness (m)*
F_{i-k}	*Radiation view factor for surface i seeing surface k*
h	*Convective heat transfer coefficient ($W/(m^2. K)$)*
g	*Acceleration of gravity (m/s^2)*
k	*Thermal conductivity (W/(m. K))*
Q	*Rate of heat transfer (W)*
q"	*Rate of heat transfer per unit area (W/m^2)*
Re	*Reynolds number*
C_p	*Specific heat capacity (J/(kg. K))*
Q_i	*Total heat transfer (W)*
$Q_{r\text{-}in(i)}$	*Solar radiation entering the room through the windows*
RH	*Relative humidity percentage*
T_{air}	*Inside air temperature (K)*
T_{out}	*Outside air temperature (K)*
T_i	*Inner wall temperature (K)*
α	*Absorptance*
ε	*Emissivity*
σ	*Stefan-Boltzmann constant*
ρ	*density (kg/m^3)*
μ	*Dynamic viscosity (kg/(m.s))*
a	*Thermal diffusivity (m^2/s)*
$Q_{c(i)}$	*Sum of the convection and conduction heat transfers (W)*
$Q_{r\text{-}out(i)}$	*Incident solar radiation to the external surface*

1. Introduction

Energy optimization and saving are the crucial goals in today's construction industry to reduce energy sources and consumption costs in building applications. Previous researches have indicated that 45% of primary energy sources are consumed by buildings, making it the single largest energy consumption sector worldwide [1]. This highlights the necessity of acquiring effective methods for energy saving in construction applications.

There are several methods to reduce energy consumption in the building industry. Many researchers have been performed to invent new constructional materials that enhanced the thermal or load performance of building constructions [2–4]. One of the methods of energy optimization is the use of phase change materials (PCM), such as organic (paraffin, non-paraffin), inorganic (salts hydrate, metallic), and eutectic (organic-organic, inorganic-inorganic and organic-inorganic) that are made alone or in combination with other construction materials [5–7]. In most cases, the combination and PCMs and other construction materials were through direct incorporation, immersion, shape stabilization, and encapsulation, to form a stable composite. The main feature of PMC's materials is to elevate the thermal energy storage capacity of building elements, as support of isolation and prevention of thermal energy dissipation [8–10].

Among the most recent research and methods for building insulation and temperature effects [11], the use of mineral insulating material, such as thermal radiation barriers in paints is a method to create cool coatings [12,13]. Also, nanomaterials have proven to be a promising candidate for the thermal insulation of buildings [14]. In the thin-walled coatings with high reflection and low absorption coefficient, the surface absorbs less solar radiation; hence, the surface temperature reduces compared to the normal case. The use of nanoparticles may improve the performance of the thermal barrier nanocomposite coatings from the heat transfer point of view [15–17]. There is not enough investigation in the thermal modeling of such coating, while there have been many studies on thermal insulations and their effect on sun energy consumption [18].

The results of some previously performed thermal analyses of light aluminum standing seam roofing systems (LASRS) showed that the thermal performance of a roofing system with a polyurethane insulation cover was better than that of lightweight roofs with glass wool insulation [19]. The results suggested that using lightweight roofs and white-colored polyurethane insulation caused a 20% reduction in the space cooling load of the building.

Another solution to reduce the surface temperature is using cool materials. The cooling effect is due to the reflection of the incident solar radiation and the emissivity of the surface. These lead to significant benefits for the buildings and the environment, including CO_2

reduction. Also, the cool materials decrease the urban heat island effect, reduce the cooling energy consumption and improve the internal thermal comfort conditions for the spaces that have not been conditioned. This concept has been utilized for white color roof materials with high reflectance [20–25]. Gagliano et al. performed a numerical comparison analysis of environmental and energy performance with the standard roof, cool roof, and green roof. The results showed that for energy savings and environmental benefits, green and cool roof utilizations are better than the standard roof [26].

In addition, an experimental investigation was implemented by Joudi et al. to study the effect of highly reflective coatings on the energy efficiency of buildings. In this study, the influence of surface radiation characteristics of highly reflective coil-coated steel cladding material on the energy efficiency features of buildings was examined by measuring the energy consumption and temperature of several test cabins having diverse interior infrared reflectivity and exterior solar reflectivity. Their results demonstrated considerable energy savings in the test cabins due to the use of highly infrared-reflective inner surfaces both during cooling and heating periods, as well as a highly reduced cooling demand by the use of high solar reflective exterior surfaces [27].

The effect of passive cooling techniques on the thermal performance of steel roofs was studied numerically by Kabore et al., where they investigated two configurations consisting; with and without an attic under tropical climate conditions. Radiant barriers, insulation cool paint, and ventilation were studied, and for both configurations, the reflective surface performed very well. However, in the attic case, due to its shape and design, and the climatic conditions, ventilation was not well [28].

The reflective cool roofs under aerosol-burdened skies were studied across some selected Indian cities by Millstein and Fischer. According to their investigations, using reflective surfaces is an inexpensive way to decrease solar loads in urban regions. Despite the high amounts of local aerosols, the results showed that cool roofs provided remarkable radiative advantages in all of the locations considered. Finally, they identified that decreasing the aerosols of the atmosphere could improve the radiative advantages of cool roofs by 23–74% [29].

Focusing on evaluating the energy loss through the cover of a room, infrared thermography of thermal bridges in building cover was carried out experimentally by Bianchi et al. [30]. The thermal transmittances of walls, ceiling, and roof were simultaneously recorded while each element was specified by its thermal insulation capability. As a reliable tool, the thermography assessment was used to quantify the incidence of thermal bridges in the building envelopes.

The effect of new roof cool tiles on indoor thermal conditions was investigated by Pisello et al. The results of their study were compared with the traditional roof brick tiles. They provided the interior thermal profiles for the roof with innovative cool clay and traditional brown brick tiles. The results showed that the inside and outside air temperature differences for the innovative cool roof case and that of the conventional roof in the summer was 2.79 K and in the winter was 1.54 K [31].

Sheikhzadeh et al. studied the effect of mineral micro particles in coatings in acrylic paints, on heat transfer and temperature distribution in a room with a cool wall, as a cooling panel, under various states and climates. They showed that acrylic paint containing mineral microparticles acts as thermal insulation, resulting in a 20% reduction in energy consumption. Also, the utilization of cooling panels and the use of mineral microparticles on external walls gives better results for hot and dry as well as hot and humid weather conditions [32].

Mohamed et al. [33] studied the effectiveness of applying radiant barrier reflective roof and interior surfaces radiation properties to reduce the space cooling loads and electricity demand of houses. Their energy simulation study indicated that the utilization of external roof coatings, internal coatings, and radiant barriers significantly reduces the cooling load in comparison to the atypical roof finish of houses.

Reilly and Kinnane studied new methods to measure the effect of thermal mass on the required energy for the heating and cooling of buildings. They have found implications for the construction design in cold climate conditions, which contradict the assumption that high thermal mass is correlated with low energy consumption. They also performed other analyses for different ranges of locations, wall types, and occupancy patterns, which led to similar results [34].

In another work, Rehman [35] evaluated the performance of bulk concrete and dry insulation materials used in passive buildings exposed to hot and humid climates. This work aimed to determine the heat flux reduction as well as the energy savings achieved in different solar radiation insulating materials. The energy was saved up to an average of 7.6–25.3% due to heat flux reduction by an average of 22–75% at the south wall during the summer period.

Most of the previous investigations on the utilization of cooling panels in buildings deal with thermal comfort, cooling capacity improvement, efficiency, and energy consumption reduction. Moreover, several studies have been performed on the thermal performance of lightweight roofs, energy efficiency of internal and external thermal insulation systems, assessment of passive cooling methods, and heat transfer issues. There are some investigations on the heat insulation effect [36] and thermal degradation kinetics for nano-clay, nano aluminum oxide (Al_2O_3), and nano zirconium oxide (ZrO_2) in polyurethane powder coatings [37,38], however, there has been no investigation on the utilization and thermal modeling of polyurethane thin layer nanocomposite coatings that contain nano aluminum oxide (Al_2O_3) and nano zirconium oxide (ZrO_2) as thermal barriers.

In another study, novel functionalized boron nitride nano-sheets (BNNS)/epoxy composites with advanced thermal conductivity and mechanical properties were studied [39]. Also, a molecular dynamics study on the thermal and rheological properties of BNNS/epoxy nanocomposites was investigated [40].

It is also common to use nanoparticles in liquid systems to investigate heat transfer. In this area some research were have done about entropy analysis of radiative hybrid nano liquid with variant thermal conductivity, thermal gradient direction on heat exchange between a pure fluid and a nanofluid, computational analysis of radiative Williamson hybrid nanofluid, and modeling for heat transfer optimization for nanoparticles in liquids [41–44].

In some studies, heat, and mass transfer have been numerically studied using magneto-hydrodynamic (MHD) by different laws and theories [45–48].

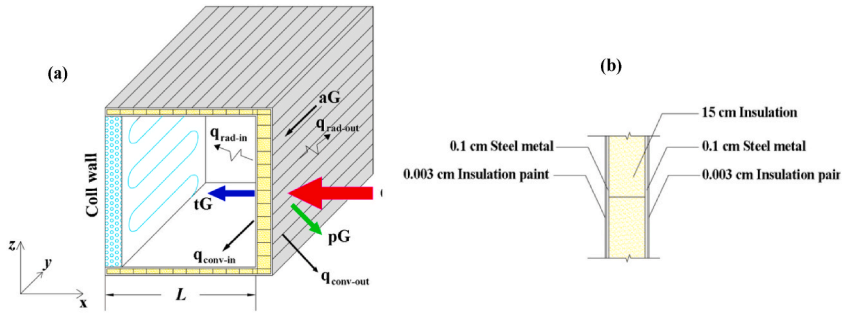

Fig. 1. (a) the geometry of the room, and (b) the configuration of the walls.

Table 1
Thermal conductivity, diffusivity, specific heat, and density of the pure polyurethane and the polyurethane nanocomposite coatings [51].

Samples	Density ρ(g/cm^3)	Specific Heat C_P (J/g.K)	Thermal Diffusivity a (cm^2/s)	Thermal Conductivity K [W/(m.K)]
Blank (PU)	1.47	1.02	0.00342	0.513
PU-3% nano ZrO_2	1.455	1	0.00292	0.425
PU-3% nano Al_2O_3	1.42	0.8	0.00341	0.388

Table 2
Overall heat transfer coefficients [W/(m^2.K)].

Coating type (On both sides)	Floor	Roof	Walls
Acrylic paint	0.227	0.2216	0.2237
Blank - 0%	0.227	0.2286	0.2307
PU- 3% nano ZrO_2	0.227	0.2287	0.2308
PU- 3% nano Al_2O_3	0.227	0.2287	0.2308

In this study, in addition to utilizing polyurethane foam inside the sandwich panels to reduce thermal conductivity, a numerical study is done to investigate the effects of applying polyurethane nanocomposite coatings on the internal and external surfaces of these panels as a thermal barrier. By using the experimental data of the study by the same author [49], a simulation of a three-dimensional room cooled by a wall radiant cooling panel with sandwich walls has been developed, to study the effect of such coatings on the internal and external surfaces as a thermal barrier on energy consumption and thermal comfort. A thermal performance evaluation has been performed on a single sunny day during the hot season in the city of Tehran, Iran. In addition, the results were compared with the data obtained from the pure polyurethane and acrylic paint coatings.

2. Research methodology

2.1. Problem definition

In the numerical simulation, a room of $3 \times 3 \times 3$ m^3 has been considered as a standard small room with sandwich panel walls coated on both sides, as shown in Fig. 1(a). The room was located on the ground with a cool western wall, while it was in contact with outside air via other walls. Given the importance of the radiation properties of the inner surfaces when radiation cooling is used, this research employs the cool-wall method, which helps in understanding the role of coating on the inner walls. The detailed configuration and materials of the walls, roof, and floor are shown in Fig. 1(b).

The external and internal coatings were made of pure polyurethane, acrylic paints, and polyurethane nanocomposite with 3% w/w Al_2O_3 and ZrO_2. The thermal conductivity, specific heat capacity, and density of the pure polyurethane and the polyurethane nanocomposite coatings were measured using a Laser Flash Analyzer device (LFA) 1000/1000 HT model (Germany). The LFA 1000 was prepared for temperatures ranging from room temperature (RT) up to 1523.15/1873.15 K and −148.15 Kup to 773.15 K. The highest accuracy was measured at ±2.2% for the thermal diffusivity, ±4% for the specific heat, and ±5% for the thermal conductivity, while the repeatability was recorded at ±2% for the thermal diffusivity, ±3.5% for the specific heat, and ±4% for the thermal conductivity. The LFA runs in agreement with national and international standards ASTM E−1461-13 [50], while it covers the widest measuring range as; 0.1 up to 2000 W/(m.K) for the thermal conductivity, as well as 0.01up to 1000 mm^2/s for the thermal diffusivity. The measurements in the experimental section were performed at least five times per sample, while the average and the standard deviations of the results have been reported. Experimental results for thermal conductivity, density, and specific heat capacity of the purely prepared polyurethane and 3% w/w Al_2O_3 and ZrO_2 nanocomposite coatings have been presented in Table 1.

It should be noted that in the experimental part various samples with different percentages of nanoparticles were prepared, and the necessary tests were made to obtain radiation and thermal conductivity coefficients as well as thermal imaging. The results of these tests showed that the optimum amount of nano oxide was 3%, therefore, the modeling was done based on it [49,51].

Table 3
The simulation parameters [30].

Parameter	Value/unit
Outdoor air temperature	$T_{out} = 309.15$ K
Ground temperature	$T_g = 291.15$ K
Acceleration of gravity	$g = -9.8$ m/s^2
Air thermal expansion coefficient	$\beta = 0.00365$ 1/K
Air viscosity	$\mu = 1.7894 \times 10^{-5}$ kg/(m.s)
Air specific heat	$c_p = 1006.43$ J/(kg.K)
Air absorption coefficient	$a = 0.2$
Air thermal diffusivity	$\alpha = 3 \times 10^{-5}$ m^2/s

Table 4
Emissivity of nanocomposite coatings in the long wavelengths (IR) [36,49].

Samples	Emissivity coefficient in IR region (ε)
Blank (PU)	0.86
PU- 3% nano ZrO_2	0.88
PU- 3% nano Al_2O_3	0.87
Acrylic paint	0.90

Concerning the configuration of the walls shown in Fig. 1(b) and based on the measured conductivity values presented in Table 1, as well as the thermal conductivity of 0.036 W/(m.K) of the sandwich panel [52], the corresponding overall heat transfer coefficients were obtained as listed in Table 2. It is worth mentioning that, a larger amount of Al_2O_3 and ZrO_2 nanoparticles in polyurethane decreases the thermal conductivity of the coating. However, the different thermal conductivity values of the coatings presented in Table 1 would have no significant effect on the overall heat transfer coefficient of the roof and the walls since the coating thickness is only 0.004 cm.

The correct and proper boundary conditions of the room's interior surfaces are important factors in the modeling and analysis of the temperature distribution in the room. These boundary conditions are usually given as temperature or heat flux, which is approximately set regarding the inside and outside conditions. To have a close approximation, using a lumped model based on the energy balance for each surface and taking into account the effects of conduction, convection, and radiations (as instructed in the published literature [32]), the model consists of convection and radiation heat transfer terms that are given as equation (1).

$$h_i A_i (T_{air} - T_i) + \varepsilon_i \sigma A_i \left\{ \sum_{k=1}^{N} F_{i-k} \left(T_k^4 - T_i^4 \right) \right\} = Q_i \tag{1}$$

where, h_i is the convection heat transfer coefficient; A_i is the surface area, T_{air} is the temperature of room air, T_i is the temperature of the i-th surfaces, T_k is the temperature of the k-th surfaces, ε_i is emissivity, $\sigma = 5.67 \times 10^{-8}$ W/(m^{2}K^4) is the Stefan-Boltzman constant, $F_{i\text{-}k}$ represents the view factor between the i-th and k-th surfaces and Q_i is total heat transfer (W).

The total heat transferred from the i-th surface is represented by the term Q_i as equation (2).

$$Q_i = Q_{c(i)} - Q_{r-in(i)} - Q_{r-out(i)} \tag{2}$$

where Q_i: *Total heat transfer (W),* $Q_{c(i)}$ is the sum of the convection and conduction heat transfers from the i-th wall. $Q_{r\text{-}in(i)}$ represents the solar radiation entering the room through the windows of the i-th wall. $Q_{r\text{-}out(i)}$ is the incident solar radiation to the external surface of the i-th wall. Since there is no window in the present case study, $Q_{r\text{-}in(i)}$ is considered zero. The energy balance for the internal surfaces of the building could be computed using equation (3).

$$Q_{c(i)} = \left(\frac{T_i - T_{out(i)}}{\frac{b_i}{k_i} + \frac{1}{h_{out(i)}}} \right) A \tag{3}$$

where $Q_{c(i)}$ is the sum of the convection and conduction heat transfers from the i-th wall. T_i is the inner wall temperature, $T_{out(i)}$ is outside air temperature, b_i is the wall thickness, k_i is thermal conductivity, $h_{out(i)}$ is the convective heat transfer coefficient and A is the area beside the internal surfaces. The energy balance for the inside air is calculated using equation (4).

$$m_{inf} C_{P,air} \left(T_{air} - T_{inf} \right) = \sum_{i=1}^{N} h_i A_i (T_i - T_{air}) \tag{4}$$

where m_{inf} is infiltration air mass flow C_p is specific heat capacity, T_{air} is inside air temperature, T_{inf} is infiltration air temperature, h_i is convective heat transfer coefficient and A_i is area and T_i is the inner wall temperature.

Table 5
Absorption coefficient in the short wavelengths (UV/VIS/NIR) region [36,49].

Samples	Absorption coefficient (α)
Blank (PU)	0.23
PU- 3% nano ZrO_2	0.19
PU- 3% nano Al_2O_3	0.19
Acrylic paint	0.40

Table 6
Intensities of solar radiation on the walls (W/m^2).

Eastern Wall	Western Wall	Roof	Northern Wall	Southern Wall
677	676	809	115	404

Table 7
Temperature of the interior surfaces (K).

Sample	Nanoparticle	Eastern wall	Western wall	Roof	Floor	Northern wall	Southern wall
C1	0%	294.69	292	294.74	294.31	294.63	294.68
A3	3% Al_2O_3	294.61	292	294.63	294.24	294.54	294.61
Z3	3% ZrO_2	294.61	292	294.61	294.24	294.52	294.61
Acrylic paint		294.86	292	295.09	294.39	294.74	294.78

Table 8
The effect of cell numbers on the total and radiation heat transfer for the case of pure polyurethane coating.

Surface Division	Number of Cells	Total heat transfer rateQ_{total} (W)	Radiation heat transfer rate$Q_{radiation}$ (W)
20 × 20 × 20	8000	130.5	105.2
30 × 30 × 30	27,000	135.1	105.6
40 × 40 × 40	64,000	133.7	105.7
50 × 50 × 50	125,000	143.8	104.6
60 × 60 × 60	216,000	154.6	105.1
80 × 80 × 80	512,000	156.8	104.4

2.2. Boundary conditions and modeling parameters

The outdoor summer design temperature, ground temperature, and physical properties of air (including specific heat, thermal expansion coefficient, thermal conductivity, dynamic viscosity, and density at 300 K) are listed in Table 3. Emissometer/Reflectometer AZ-Technology's TEMP 2000A and Shimadzu spectrophotometer UV-3600 were used to measure the emissivity and reflection coefficient of the samples [49].

The absorption coefficient and surface emissivity, respectively, for acrylic paint, pure polyurethane, and innovative nanocomposite coatings at their best composition, i.e., 3% w/w Al_2O_3 and ZrO_2 [49], are listed in Tables 4 and 5. The results presented in Tables 4 and 5 have been used for the energy balance and the results presented in Table 5 have been used for modeling the internal conditions.

Based on the conditions mentioned above, the Rayleigh number is greater than 10^{10} and, hence, the fluid regime is turbulent. Since the air velocity of air is low enough in the room, the flow is considered incompressible. To determine the velocity and temperature fields, the governing equations have to be solved for the steady, incompressible flow in a three-dimensional Cartesian coordinate. The governing equations are the continuity, momentum, turbulence, and energy equations that are coupled through the buoyancy term. This was done using the Fluent software and by employing the SIMPLE algorithm to accommodate the pressure-velocity coupling and k-ε (RNG: Renormalization group) to model the turbulence. In addition, due to low-temperature gradients, use of the Boussines q approximation with $\rho = 1.22 \frac{kg}{m^3}$ is utilized. Also due to low optical thickness (aL< 1) and low-temperature gradients, the DO radiation model has been employed [49,53].

By utilizing an overall energy balance, a computer code was prepared to obtain the walls' interior surface temperatures. For this purpose, the highest intensities of solar radiation on the walls, calculated by the Carrier software were considered, and the results have been presented in Table 6. The interior surface temperatures for different coating cases have been presented in Table 7.

The results for the cooling panel temperature of 292.15 K [32] and outdoor summer design temperature of 309.15 K on an August sunny day at 1:00 p.m. in the city of Tehran, Iran, as a hot and sunny day in summer were obtained.

2.3. Grid system selection and refinement

In order to minimize the computational time, the structured mesh was used in the simulation of the room. In addition, adaptive meshing with an expansion coefficient of 1.05 was used to apply an accurate heat transfer effect near the boundaries [54]. Several grid systems were tested to ensure the mesh independence of the results and to determine the appropriate number of cells. The results for

Table 9
Internal surface temperatures (K); Results of the computer code of this study and those presented in Rahimi and Sabernaeemi's study [55].

	Northern	Southern	Eastern	Western	Roof	Floor
Experimental work	295.6	295.5	295.7	295.6	295.8	300.7
The present study	296.9	296.9	296.9	296.9	296.9	300.7

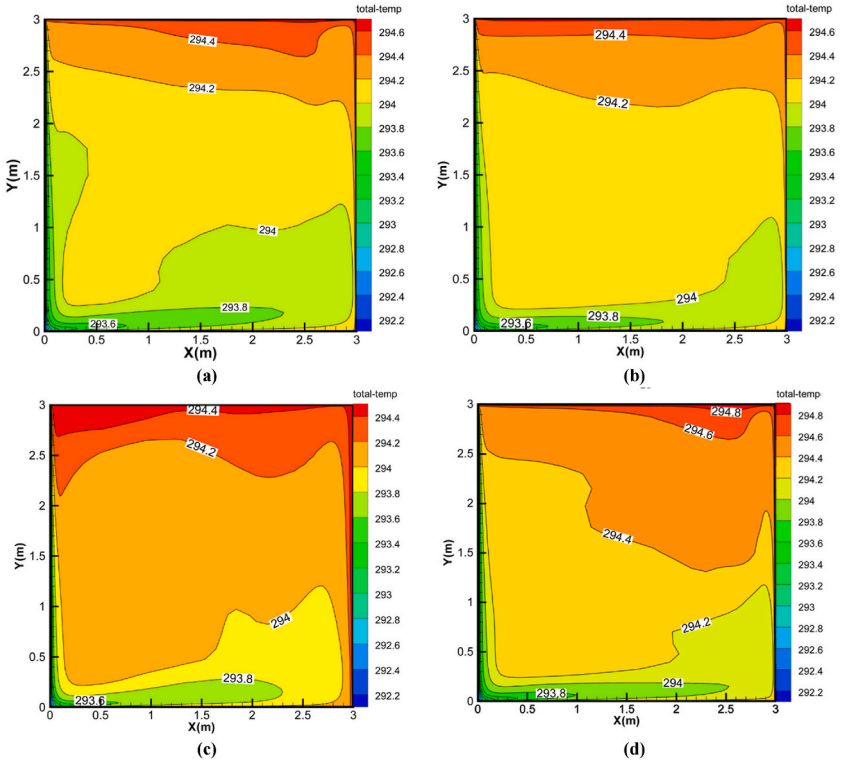

Fig. 2. Isothermal lines on XY plane and at Z = 1.5 for different cases. a) Case 1: pure polyurethane coating, b) Case 2: Al_2O_3 nanocomposite coating, c) Case 3: ZrO_2 nanocomposite coating and d) Case 4: Acrylic paint. (Temperatures are in K).

the total and radiation heat fluxes, utilizing different grid systems, are presented in Table 8 (for the case in which pure polyurethane coating on the walls is used). Results indicated that the total heat transfer rate changed by less than 2% when the grid system with more than 512,000 cells was considered in comparison to 216,000. Therefore, the grid system of 216,000 cells was used in the models.

2.4. Validation

In order to validate the developed code for obtaining the temperature of the interior surfaces, the simulation of the sample in an experiment developed by Rahimi and Sabernaeemi [55] was implemented with the assumption of similar boundary conditions. In this regard, the interior surface temperatures calculated using the code were compared with the experimental results, as reported in Table 9 [55]. The comparison shows a good matching with a maximum relative difference of about 0.4%.

3. Results and discussion

3.1. Results of the simulation

Several simulations have been run for the case studies that used pure polyurethane, acrylic paint, and polyurethane nanocomposite with 3% w/w Al_2O_3 and ZrO_2 nanoparticles coatings on the internal and external room surfaces.

Under the same environmental conditions and solar radiation in summer, as observed from Table 7, a lower internal surface temperature for the walls with nanocomposite coatings including Al_2O_3 and ZrO_2 has been obtained, when compared with the walls without these coatings. This difference is due to lower absorption and higher reflection by the walls with the aforementioned coatings, which remarkably reduce the heat loss through the walls. Fig. 2 shows the temperature distribution on the vertical plane in the middle of the room for the following four coating cases on both sides: the wall with a pure polyurethane coating, the wall with Al_2O_3 nanocomposite coating, the wall with ZrO_2nanocompositecoating, and the wall with acrylic paint.

Although, the temperature distributions have shown some differences in detail of the four cases, however, the temperature values

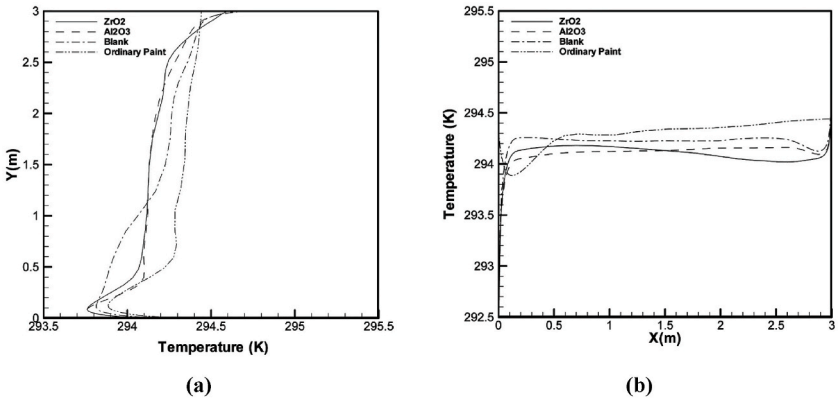

Fig. 3. Vertical (a) and horizontal (b) temperature profiles in the middle of the room for different cases.

Table 10
Heat transfer rate through the walls (W).

Coating (On both sides of the wall)	Total heat transfer rate	Radiation heat transfer rate
Acrylic paint	171.95	118.59
Blank (PU)	154.62	105.13
PU- 3% nano ZrO_2	150.38	103.94
PU- 3% nano Al_2O_3	150.92	103.21

were within the thermal comfort range as instructed in the literature [56]. It should be noted that the simulation is done in three-dimension and the surfaces are considered with constant temperature boundary conditions. At the same time, the heat transfer from the walls depended on the surrounding air inside the room. For a better comparison, the temperature distribution in the room's central location in the horizontal and vertical directions (four cases) is extracted, as shown in Fig. 3.

The detail of temperature distribution on the vertical and horizontal centerline is distinct (Fig. 3), however, the lowest temperatures are for the Al_2O_3 or ZrO_2 nanocomposites. Furthermore, there is almost a 0.5 °C temperature decrease for Al_2O_3 and ZrO_2 nanocomposites coatings compared with acrylic paint, which results in lower energy consumption.

To select the best coating performance, the total heat transfer rate through the walls, as well as the radiation heat transfer rate from the internal surfaces is obtained as presented in Table 10. The lowest heat load is related to the nanocomposite coating with nano ZrO_2. The nanocomposite coatings containing ZrO_2 and Al_2O_3 have the same thermal performance and demonstrate less than a 0.5% difference in heat loss. Compared to pure polyurethane coatings and acrylic paints, nanocomposite coatings with ZrO_2 yield 4% and 13% fewer energy consumptions, respectively. This indicates the significant influence of composite coatings in general and the ZrO_2 nanocomposite coating on energy consumption reduction. One of the important results of this study, in which a wall was utilized as a radiant cooling panel, is that the share of radiation heat transfer from the internal surfaces is at least 64% for acrylic paint and at most 70% for ZrO_2 nanocomposite coating. These results indicate the effective role of nano zirconium oxide and aluminum oxide nanoparticles in lower absorption and higher reflection effect on surface coatings and preventing heat transfer, which is consistent with experimental results.

3.2. Thermography results of the samples

To evaluate the radiation performance of the case studies, the experimental thermography of the samples was performed. For this purpose, they were placed outdoors horizontally under the incident of solar radiation. Because the coating was designed to reduce the absorption coefficient and increase the emission coefficient at low wavelengths, the imaging was carried out on a hot and sunny day in summer. For modeling, the weather data of the same day was used according to the Meteorological Center report. Using an infrared camera, 10 × 15 cm coated plates were imaged on 15th August at 12 p.m. Fig. 4 shows the temperature variations along with the line P of the samples.

Despite similar environmental conditions and solar radiation, the average temperatures of the sample with a pure polyurethane coating, Al_2O_3 nanocomposite coating, and the sample with ZrO_2 nanocomposite coating were 309.35 K, 309.25 K, and 307.15 K, respectively. The 2-degree difference in temperature indicates a higher radiation reflection of the nanocomposite coating with ZrO_2 coating. The difference in the temperature of the coating used with zirconium nano oxide and aluminum oxide nanoparticles indicates that the coating that contains zirconium nano oxide has a greater effect on reducing absorption and increasing the reflection, which is related to its inherent nature. In other words, this coating, with lower absorption and higher radiation reflection, significantly reduces the thermal losses through the building walls.

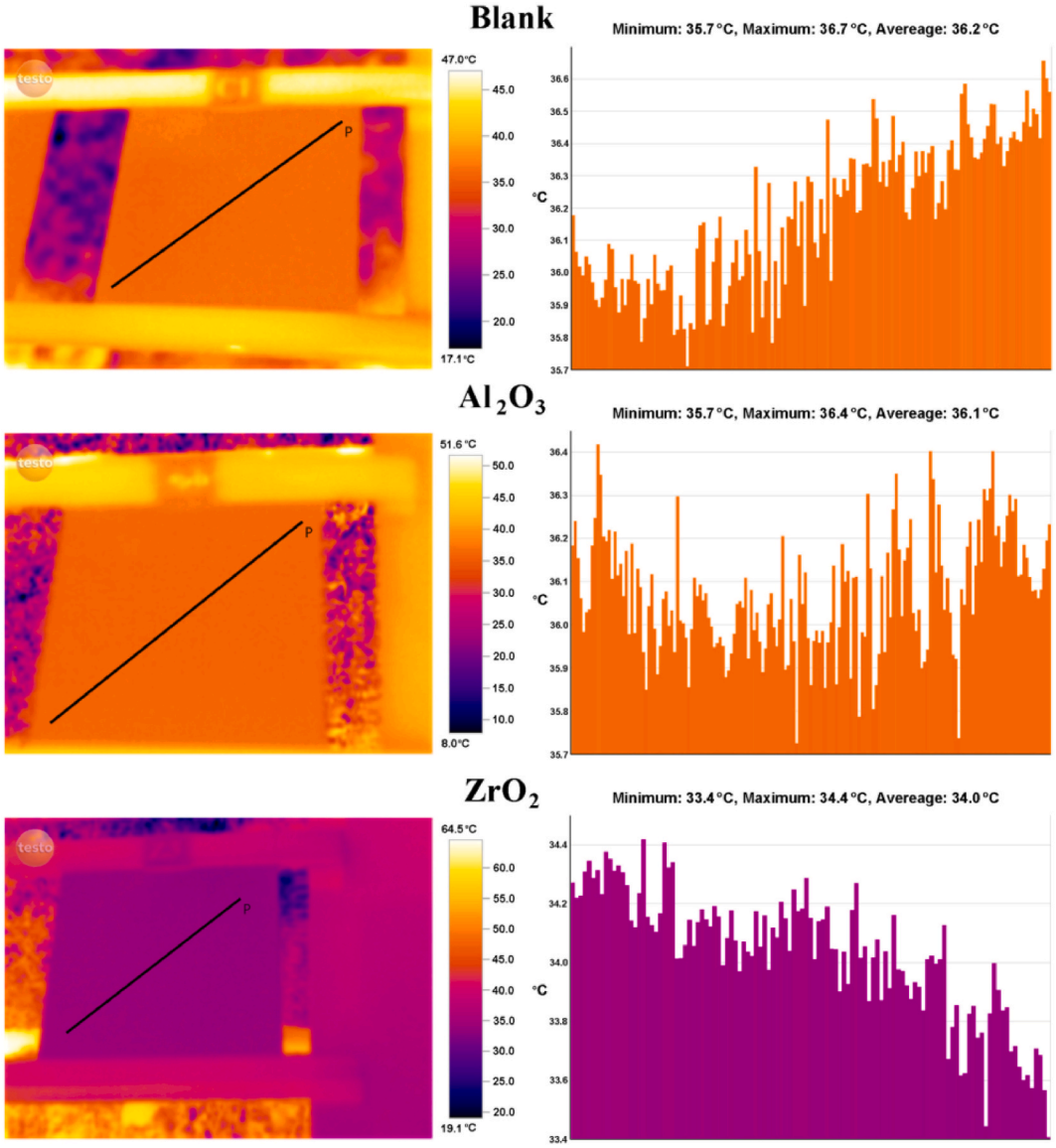

Fig. 4. Thermal image of the sample coated with pure polyurethane and 3% w/w Al_2O_3 and ZrO_2 nanocomposites.

4. Conclusions

The insulation of building outside walls by thermal barrier coating is introduced as a new approach that significantly reduces the energy consumption in buildings. In this study, a numerical approach and experimental assessment are used to investigate the effects of coated polyurethane nanocomposite "containing nano Al_2O_3 and nano ZrO_2 on both sides of the walls of a sample room" on temperature distribution and heat transfer. The following are the results in brief.

- For all the studied cases, despite the cold wall with a constant temperature of 292 K, the temperature is within the comfort range.
- The measured thermal conductivity of the nanocomposite coatings having 3% w/w Al_2O_3 and ZrO_2 decreased by 24% and 17% compared to that of pure polyurethane, respectively.
- ZrO_2 and Al_2O_3 nanocomposite coatings showed almost the same thermal performance and had than 0.5% discrepancy in thermal loss with respect to each other.
- The nanocomposite coatings applied on both sides of the room walls acted as thermal barriers. The results showed that nanocomposite coatings, compared to pure polyurethane coatings and acrylic paints, reduced the thermal losses by 4% and 13%, respectively.
- With the utilization of the western wall as the radiant cooling panels, thermal radiation was the dominant heat transfer mechanism and it was at least 64% and at most 70%.

- Regarding the low absorption coefficient of ZrO_2 and Al_2O_3 nanocomposite coatings, their utilization on the walls of the sandwich panels for hot-dry and hot-humid climates in regions with long summers and high solar radiation seem appropriate.
- It was observed that the walls with nanocomposite coating of 3% w/wZrO_2 improve the performance of the radiant cooling panel by about 12%, also reducing energy consumption.

Authors contributions

Conceptualization, Software, Data curation, and Writing - original draft: *A.A.Azemati, S.S.R.Koloor, and B.S.Hadavand.*

Formal analysis, Investigation, Methodology, Validation, Visualization, Writing - review & editing: *A.A.Azemati, S.S.R.Koloor, H. Khorasanizadeh, G.A.Sheikhzadeh, B.S.Hadavand, M.Eldessouki.*

Funding acquisition, Project administration, Resources, Supervision: *S.S.R.Koloor, B.S.Hadavand, M.Eldessouki.*

All authors have read and approved the final version of the article.

Declaration of competing interest

The authors declare that they have no known competing financial interests or personal relationships that could have appeared to influence the work reported in this paper.

Data availability

Data will be made available on request.

Acknowledgment

The authors acknowledge funding from the European Union's Horizon 2020 research and innovation program under the Marie Sklodowska-Curie grant agreement No 834966. The research was also supported by the Ministry of Education, Youth, and Sports of the Czech Republic and the European Union (European Structural and Investment Funds Operational Program Research, Development, and Education) in the framework of the project "Modular platform for autonomous chassis of specialized electric vehicles for freight and equipment transportation", Reg. No. CZ.02.1.01/0.0/0.0/16_025/0007293, as well as the support of the Minister of Transport and Construction of the Slovak Republic and the European Union in the transport sector and Information Technology in the frames of the project "Adaptation of 21st century technologies for non-conventional low-emission vehicles based on composite materials ", Reg. No. NFP313010BXF3 by OPII – VA/DP/2021/9.3 -01.

References

[1] G. Pérez, et al., Green facade for energy savings in buildings: the influence of leaf area index and facade orientation on the shadow effect, Appl. Energy 187 (2017) 424–437.
[2] S.E. Mohammadyan-Yasouj, et al., Thermal performance of alginate concrete reinforced with basalt fiber, Crystals 10 (9) (2020) 779.
[3] A.M. Saba, et al., Strength and flexural behavior of steel fiber and silica fume incorporated self-compacting concrete, J. Mater. Res. Technol. 12 (2021) 1380–1390.
[4] M. Joshani, et al., Damage mechanics model for fracture process of steel-concrete composite slabs, in: Applied Mechanics and Materials, Trans Tech Publ, 2012.
[5] A. Mistri, et al., A review on different treatment methods for enhancing the properties of recycled aggregates for sustainable construction materials, Construct. Build. Mater. 233 (2020), 117894.
[6] H. Shokravi, et al., Effect of alumina additives on mechanical and fresh properties of self-compacting concrete: a review, Processes 9 (3) (2021) 554.
[7] P. Rafiei, et al., Temperature impact on engineered cementitious composite containing basalt fibers, Appl. Sci. 11 (15) (2021) 6848.
[8] J. Jiang, et al., Design of a novel nanocomposite with CSH@ LA for thermal energy storage: a theoretical and experimental study, Appl. Energy 220 (2018) 395–407.
[9] S.A. Memon, Phase change materials integrated in building walls: a state of the art review, Renew. Sustain. Energy Rev. 31 (2014) 870–906.
[10] A. Sharma, et al., Review on thermal energy storage with phase change materials and applications, Renew. Sustain. Energy Rev. 13 (2) (2009) 318–345.
[11] S.E. Mohammadyan-Yasouj, et al., Experimental study on the effect of basalt fiber and sodium alginate in polymer concrete exposed to elevated temperature, Processes 9 (3) (2021) 510.
[12] A.A. Azemati, et al., Thermal modeling of mineral insulator in paints for energy saving, Energy Build. 56 (2013) 109–114.
[13] M.Z.M. Ashhar, et al., Recent research and development on the use of reflective technology in buildings–A review, J. Build. Eng. 45 (2022), 103552.
[14] M.A. Mujeebu, et al., Effect of nano vacuum insulation panel and nanogel glazing on the energy performance of office building, Appl. Energy 173 (2016) 141–151.
[15] A. Madhi, et al., UV-curable urethane acrylate zirconium oxide nanocomposites: synthesis, study on viscoelastic properties and thermal behavior, J. Compos. Mater. 52 (21) (2018) 2973–2982.
[16] Y. Zhang, et al., Recent progress in the development of thermal interface materials: a review, Phys. Chem. Chem. Phys. 23 (2) (2021) 753–776.
[17] A. Madhi, et al., Thermal conductivity and viscoelastic properties of UV-curable urethane acrylate reinforced with modified Al2O3 nanoparticles, Progress in Color, Colorants and Coatings 10 (3) (2017) 193–204.
[18] M.K. Nematchoua, et al., Application of phase change materials, thermal insulation, and external shading for thermal comfort improvement and cooling energy demand reduction in an office building under different coastal tropical climates, Sol. Energy 207 (2020) 458–470.
[19] J. Han, et al., Investigation on the thermal performance of different lightweight roofing structures and its effect on space cooling load, Appl. Therm. Eng. 29 (11–12) (2009) 2491–2499.
[20] T. Xu, et al., Quantifying the direct benefits of cool roofs in an urban setting: reduced cooling energy use and lowered greenhouse gas emissions, Build. Environ. 48 (2012) 1–6.
[21] J. Hu, et al., Adaptive building roof by coupling thermochromic material and phase change material: energy performance under different climate conditions, Construct. Build. Mater. 262 (2020), 120481.
[22] A. Synnefa, et al., Estimating the effect of using cool coatings on energy loads and thermal comfort in residential buildings in various climatic conditions, Energy Build. 39 (11) (2007) 1167–1174.
[23] H. Akbari, et al., Global cooling: increasing world-wide urban albedos to offset CO 2, Climatic Change 94 (3–4) (2009) 275–286.

[24] J. Lucero-Álvarez, et al., Effects of solar reflectance and infrared emissivity of rooftops on the thermal comfort of single-family homes in Mexico, in: Building Simulation, Springer, 2017.
[25] J. Triano-Juárez, et al., Thermal behavior of a phase change material in a building roof with and without reflective coating in a warm humid zone, J. Build. Eng. 32 (2020), 101648.
[26] A. Gagliano, et al., A multi-criteria methodology for comparing the energy and environmental behavior of cool, green and traditional roofs, Build. Environ. 90 (2015) 71–81.
[27] A. Joudi, et al., Highly reflective coatings for interior and exterior steel cladding and the energy efficiency of buildings, Appl. Energy 88 (12) (2011) 4655–4666.
[28] M. Kabore, et al., Assessment on passive cooling techniques to improve steel roof thermal performance in hot tropical climate, Int. J. Energy Power Eng. 3 (6) (2014) 287.
[29] D. Millstein, et al., Reflective 'cool' roofs under aerosol-burdened skies: radiative benefits across selected Indian cities, Environ. Res. Lett. 9 (10) (2014), 104014.
[30] F. Bianchi, et al., Infrared thermography assessment of thermal bridges in building envelope: experimental validation in a test room setup, Sustainability 6 (10) (2014) 7107–7120.
[31] A.L. Pisello, et al., Investigation on the effect of innovative cool tiles on local indoor thermal conditions: finite element modeling and continuous monitoring, Build. Environ. 97 (2016) 55–68.
[32] G. Sheikhzadeh, et al., The effect of mineral micro particle in coating on energy consumption reduction and thermal comfort in a room with a radiation cooling panel in different climates, Energy Build. 82 (2014) 644–650.
[33] H.I. Mohamed, et al., The effect of exterior and interior roof thermal radiation on buildings cooling energy, Procedia Eng. 145 (2016) 987–994.
[34] A. Reilly, et al., The impact of thermal mass on building energy consumption, Appl. Energy 198 (2017) 108–121.
[35] H.U. Rehman, Experimental performance evaluation of solid concrete and dry insulation materials for passive buildings in hot and humid climatic conditions, Appl. Energy 185 (2017) 1585–1594.
[36] A.A. Azemati, et al., Heat insulation effect in solar radiation of polyurethane powder coating nanocomposite, Sci. Rep. 11 (1) (2021) 1–9.
[37] M. Jouyandeh, et al., Thermal-resistant polyurethane/nanoclay powder coatings: degradation kinetics study, Coatings 10 (9) (2020) 871.
[38] B.S. Hadavand, et al., Silane-functionalized Al2O3-modified polyurethane powder coatings: nonisothermal degradation kinetics and mechanistic insights, J. Appl. Polym. Sci. 137 (45) (2020), 49412.
[39] Z. Liu, et al., Novel functionalized BN nanosheets/epoxy composites with advanced thermal conductivity and mechanical properties, ACS Appl. Mater. Interfaces 12 (5) (2020) 6503–6515.
[40] Z. Liu, et al., A molecular dynamics study on thermal and rheological properties of BNNS-epoxy nanocomposites, Int. J. Heat Mass Tran. 126 (2018) 353–362.
[41] W. Jamshed, et al., Entropy analysis of radiative [MgZn6Zr-Cu/EO] Casson hybrid nanoliquid with variant thermal conductivity along a stretching surface: implementing Keller box method, Proc. IME C J. Mech. Eng. Sci. (2022), 09544062211065696.
[42] A. Koulali, et al., Comparative study on effects of thermal gradient direction on heat exchange between a pure fluid and a nanofluid: employing finite volume method, Coatings 11 (12) (2021) 1481.
[43] T. Zubair, et al., Computational analysis of radiative Williamson hybrid nanofluid comprising variable thermal conductivity, Jpn. J. Appl. Phys. 60 (8) (2021), 087004.
[44] M.M. Fayyadh, et al., The mathematical model for heat transfer optimization of Carreau fluid conveying magnetized nanoparticles over a permeable surface with activation energy using response surface methodology, ZAMM-J. Appl. Mathemat. Mechanics/Zeitschrift für Angewandte Mathematik und Mechanik 102 (11) (2022), e202100185.
[45] A. Salmi, et al., Computational analysis for enhancement of heat and mass transfer in MHD-polymer with hybrid nano-particles using generalized laws, Case Stud. Therm. Eng. 31 (2022), 101851.
[46] M. Nawaz, et al., Numerical study on thermal enhancement in hyperbolic tangent fluid with dust and hybrid nanoparticles, Int. Commun. Heat Mass Tran. 127 (2021), 105535.
[47] M. Shoaib, et al., A design of soft computing intelligent networks for MHD Carreau nanofluid model with thermal radiation, Int. J. Mod. Phys. B 36 (27) (2022), 2250192.
[48] M. Shoaib, et al., Impact of thermal energy on MHD Casson fluid through a Forchheimer porous medium with inclined non-linear surface: a soft computing approach, Alex. Eng. J. 61 (12) (2022) 12211–12228.
[49] A.A. Azemati, et al., Study on radiation properties of polyurethane/nano zirconium oxide nanocomposite coatings, in: Materials Science Forum, Trans Tech Publ, 2017.
[50] A. Standard, Standard Test Method for Thermal Diffusivity by the Flash Method, E1461, ASTM International, West Conshohocken, PA, 2013, p. 10.
[51] A.A. Azemati, et al., Experimental study on thermal conductivity of polyurethane resin filled with modified nanoparticles, J. Comput. Appl. Res. Mech. Eng. 8 (1) (2018) 97–106.
[52] M.A. Joudi, Radiation Properties of Coil-Coated Steel in Building Envelope Surfaces and the Influence on Building Thermal Performance, Linköping University Electronic Press, 2015.
[53] H. Khorasanizadeh, et al., Numerical study of air flow and heat transfer in a two-dimensional enclosure with floor heating, Energy Build. 78 (2014) 98–104.
[54] J.D. Anderson, et al., in: Computational Fluid Dynamics, 206, Springer, 1995.
[55] M. Rahimi, et al., Experimental study of radiation and free convection in an enclosure with under-floor heating system, Energy Convers. Manag. 52 (7) (2011) 2752–2757.
[56] B. Olesen, Radiant floor cooling systems, ASHRAE J. 50 (9) (2008) 16–22.